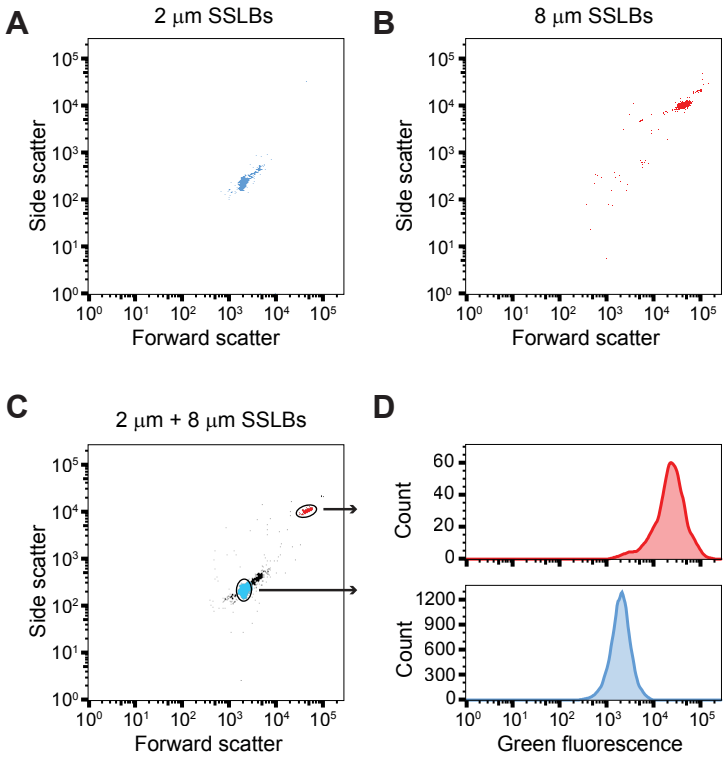

Supplementary Figure S1. Related to Figure 1. Quantification of fluorescence by flow cytometry. Forward vs. side scatter was used to distinguish SSLB populations based on size: (A) 2-μm SSLBs, (B) 8-μm SSLBs, and (C) a mixed population of 2-μm and 8-μm SSLBs. (D) Gates were drawn to quantify green fluorescence for each population.

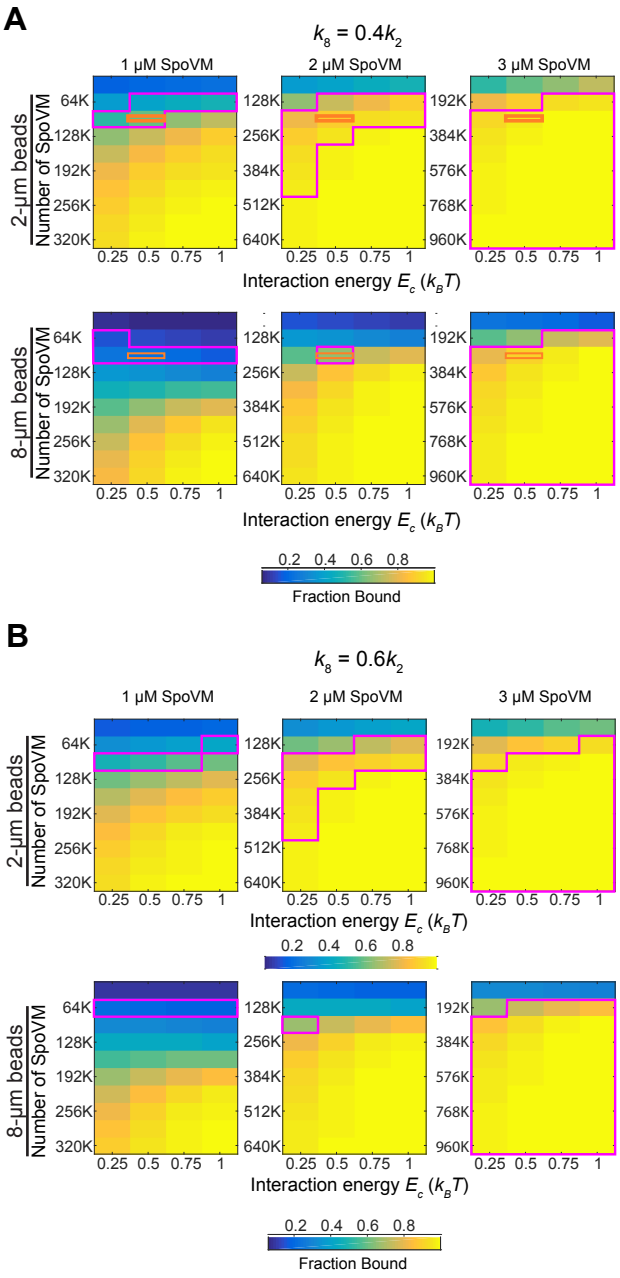

Supplemental Figure S2. Related to Figure 1. Experimental binding kinetics from Monte Carlo simulations are best fit by an on-rate ratio of k_8/k_2 = 0.5. Simulations were performed as in Fig. 3, except with k_8/k_2 = 0.4 (A) or k_8/k_2 = 0.6 (B). Across a wide range of values of the total number of SpoVM molecules (N) and the cooperativity energy E_c, we computed the normalized steady-state binding with k_8/k_2 = 0.4 or 0.6 and identified regions of parameter space (magenta) that were consistent with our experimental data (within one standard deviation of the mean) on 2- and 8-μm SSLBs for simulations with N, 2N, and 3N molecules to mimic 1, 2, and 3 μM SpoVM concentrations. The orange rectangle in (A) denotes parameters for which simulations agreed with our experimental data for both SSLB sizes and across the 3-fold concentration range; this region is smaller than for k_8/k_2 = 0.5 in Fig. 3. No such region was identified in (B).

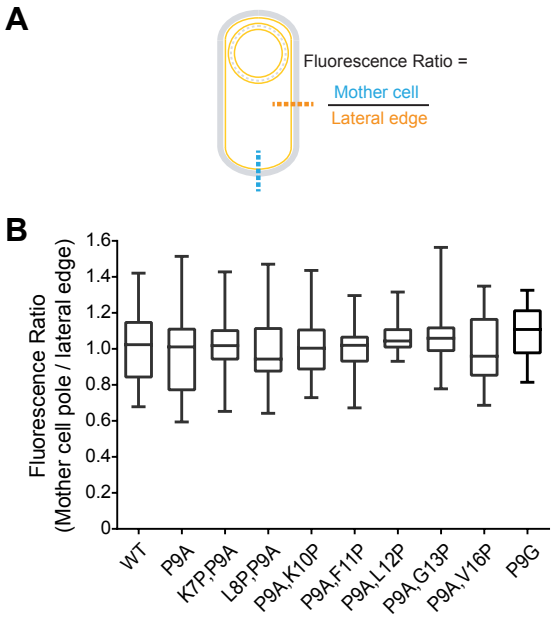

Supplemental Figure S3. Related to Figure 2. Quantification of SpoVM-GFP fluorescence intensities at the mother cell pole and along the lateral edge. (A) Schematic of sporulating *B. subtilis* and representative line scans across the mother cell pole (blue) and mother cell lateral edge (orange) membranes. (B) Ratio of pole to lateral edge membrane maximum fluorescence intensities from line scans as shown in (A) in sporulating *B. subtilis* cells producing the indicated SpoVM-GFP variants.

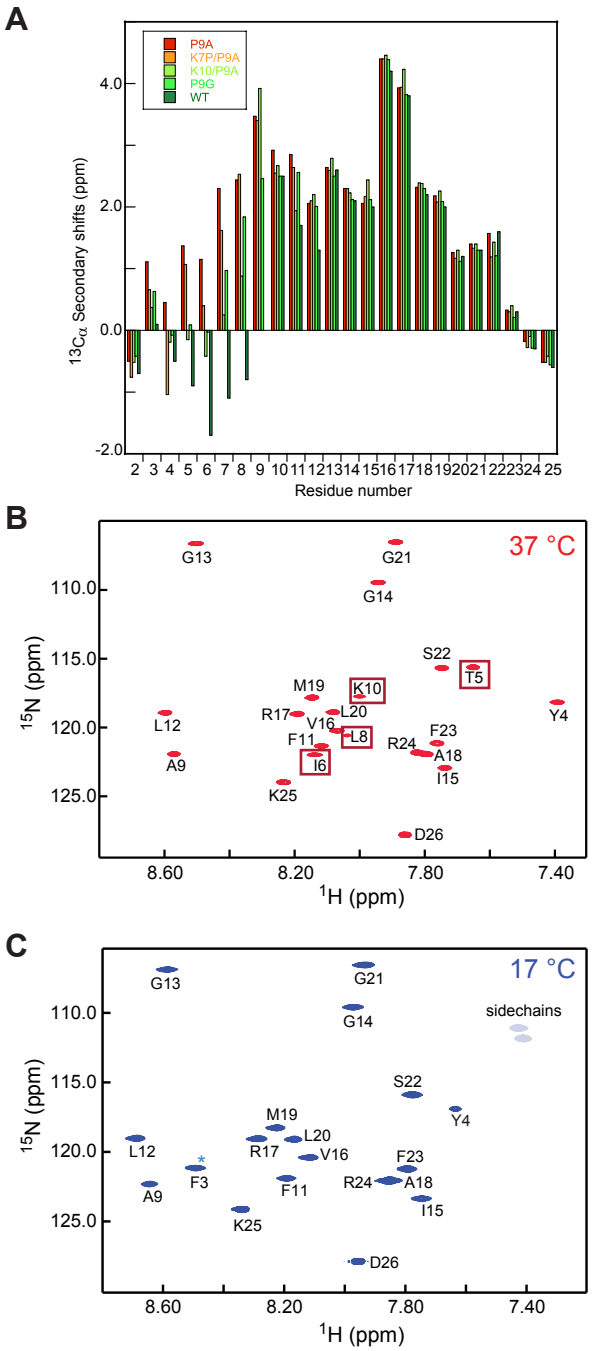

Supplemental Figure S4. Related to Figure 2. (A) ^{13}Cα secondary chemical shifts for residues 2 to 25 of SpoVM^{WT} and variants. (B,C) The 2D ^{15}N-^{1}H TROSY spectra of SpoVM^{K7P,P9A} at (B) 37 °C and (C) 17 °C. Several resonances including residues 4, 6, 8, and 10 disappear at 17 °C, indicating a conformational exchange in SpoVM^{K7P,P9A}.

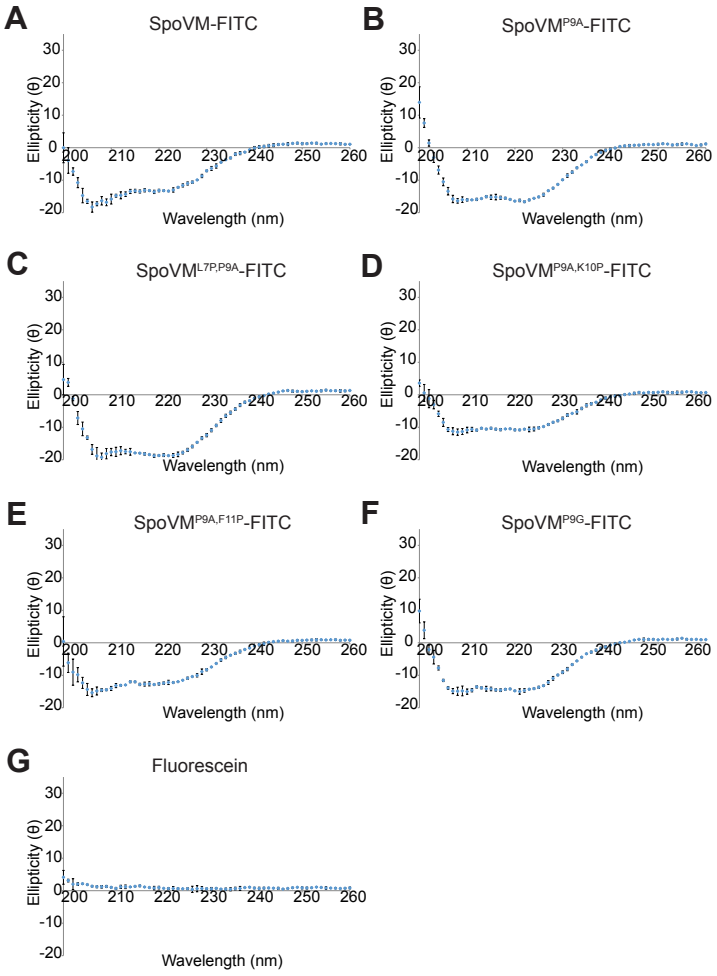

Supplemental Figure S5. Related to Figure 2. Circular dichroism spectra of FITC-conjugated SpoVM variants incubated with small unilamellar vesicles (SUVs). (A) SpoVM-FITC, (B) SpoVM^{P9A}-FITC, (C) SpoVM^{L8P,P9A}-FITC, (D) SpoVM^{P9A,K10P}-FITC, (E) SpoVM^{P9A,F11P}-FITC, (F) SpoVM^{P9G}-FITC, and (G) fluorescein. Data points and error bars represent mean values and standard deviation from the mean, respectively, from three technical replicates.

Supplemental Table S1. Related to Figure 3. Effect of Pro substitution or position on sporulation efficiency (heat resistance). Standard deviation from mean is reported in parentheses (*n*=3 independent trials). "N/A" indicates "not applicable".

Strain[a]	*spoVM*	*spoVM* allele at *amyE* locus	Sporulation efficiency (relative to WT)
A	WT	-	1
B	Δ	-	$< 2.8 \times 10^{-8}$ (N/A)
C	Δ	WT	0.58 (0.14)
D	Δ	P9A	$< 2.8 \times 10^{-8}$ (N/A)
E	Δ	K7P, P9A	$< 2.8 \times 10^{-8}$ (N/A)
F	Δ	L8P, P9A	$< 2.8 \times 10^{-8}$ (N/A)
G	Δ	P9A, K10P	$< 2.8 \times 10^{-8}$ (N/A)
H	Δ	P9A, F11P	$< 2.8 \times 10^{-8}$ (N/A)
I	Δ	P9G	0.04 (0.01)

[a]Strain A: PY79; B: KR94; C: EYKS883; D: D: EYKS884; E: EYKS917; F: EYKS918; G: EYKS885; H: EYKS886; I: EYKS909. Genotypes are listed in STAR Methods.